Evaluating the Warping of Laminated Particleboard Panels

Zhiyong Cai, Ph.D., P.E.

USDA Forest Service
Forest Products Laboratory
One Gifford Pinchot Dr.
Madison, WI 53726-2398
zcai@fs.fed.us

ABSTRACT

Laminated wood composites have been used widely in the secondary manufacturing processes in the wood panel industries. Warping, which is defined as the out-of-plane deformation of an initially flat panel, is a longstanding problem associated with the use of laminated wood composites. The mechanism of warping is still not fully understood. A new two-dimensional warping model based on mechanics of layered composites was introduced to simulate the warping behavior of laminated wood composites. Actual warping performances of veneered particleboard panels under different relative humidity environments were tested and compared with the predicted warping performances based on the two-dimensional warping model. The result indicted that the new warping model could be used to simulate the warping behavior of layered wood-based composites.

Keywords: laminated, warping, wood composite, layered, simulation.

INTRODUCTION

Laminated wood composites have been used widely in the secondary manufacturing processes in the wood panel industries. Warping of wood-based composites is a long-standing problem associated with use of laminated wood composite panels. Warping is defined as the out-plane deformation of a panel from an initially flat condition (Suchsland and McNatt 1986). Severe warping of finished products has the potential to significantly increase the cost of manufacturing and lower the consumer's confidence in using wood products. The Composite Panel Association (previously called the National Particleboard Association) considers warp to be the leading technical problem requiring further investigation (National Particleboard Association 1996).

Heebink, et al. (1964) developed a one-dimensional mathematical model by equating the strain (due to the changes in moisture content and temperature) to the strain (determined by the geometry of the panel). Many researchers (Norris 1964, Suchsland and McNatt 1986, Suchsland 1990, Suchsland, et al. 1993 and 1995, Wu 1999) have used the one-dimensional warping model to investigate warping problems in a number of wood-based composites including particleboard, laminated wood panels, veneered furniture panels, plywood, and medium density fiberboard (MDF). While this model has evolved and found continued use, it does not include the effect of lateral strain. Lateral strain is usually determined through

Poisson's ratio and needs to be considered for a two-dimensional (plane) panel. To model warping in two dimensions, the finite element method (FEM) was introduced (Tong and Suchsland 1993, and Cloutier, et al. 2001). The more recent work by Cloutier, et al. (2001) used FEM to model wood composite panels based on unsteady-state moisture transfer and mechanical equilibrium. Differing wood composites require the selection of different elements.

Composite wood panels can be regarded as a multi-layered composite material, where each layer has a unique set of physical properties. Individual layers can be approximated as an orthotropic material having two principal directions. Sun (1994) showed that the behavior of wood composites can be modeled using the mechanics of layered composites. The goal of this study is to investigate and model the warping mechanism of wood composites using the theory of mechanics in layered composites and thus provide insight into understanding the wood composite warping. A better means to model warp will provide new knowledge to help minimize warp in wood composites.

MECHANICS OF LAYERED COMPOSITES

The mechanical behavior of layered composite materials is quite different from that of most common engineering materials which are homogeneous and isotropic. The makeup and physical properties of layered composites varies with location and orientation of the principal axes. Wood has unique and independent mechanical properties in the directions of three mutually perpendicular axes, so it may be described as an orthotropic material (Wood Handbook 1999). Figure 1 shows a typical wood veneer with two principal directions that are perpendicular to each other. For thin layers, a state of plane stress parallel to the laminate can be assumed with reasonable accuracy. The two-dimensional stress-strain equation is (Sun 1994):

$$\begin{Bmatrix} \sigma_1 \\ \sigma_2 \\ \sigma_{12} \end{Bmatrix} = \begin{bmatrix} \dfrac{E_1}{1-\upsilon_{12}\upsilon_{21}} & \dfrac{\upsilon_{12}E_2}{1-\upsilon_{12}\upsilon_{21}} & 0 \\ \dfrac{\upsilon_{12}E_2}{1-\upsilon_{12}\upsilon_{21}} & \dfrac{E_2}{1-\upsilon_{12}\upsilon_{21}} & 0 \\ 0 & 0 & G_{12} \end{bmatrix} \begin{Bmatrix} \varepsilon_1 \\ \varepsilon_2 \\ \gamma_{12} \end{Bmatrix} \tag{1}$$

where 1 and 2 represent the two principal coordinate directions; E_1 and E_2 are the moduli of elasticity along the two directions; σ_{11} and σ_{22} are stresses along the two principal coordinates; σ_{12} is the in-plane shear stress; G_{12} is the in-plane shear modulus; v_{12} is Poisson's ratio measuring contraction in the *1*-direction due to uniaxial loading in the *2*-direction; v_{21} is Poisson's ratio measuring contraction in the *2*-direction due to uniaxial loading in the *1*-direction; ε_{11} and ε_{22} are strains along the two principal coordinates; and γ_{12} is the shear strain. The 3x3 matrix of elastic constants is usually denoted by:

$$[Q] = \begin{bmatrix} Q_{11} & Q_{12} & 0 \\ Q_{12} & Q_{22} & 0 \\ 0 & 0 & Q_{66} \end{bmatrix} \tag{2}$$

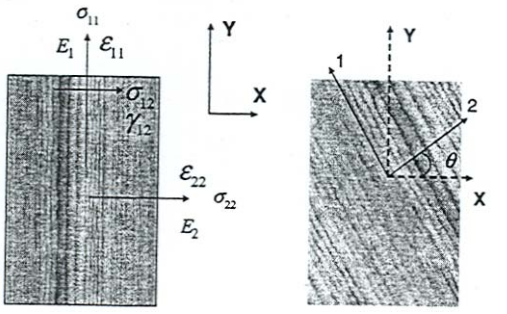

Figure 1 - Orthotropic characteristics of thin layer and its coordinates

Usually, during the construction of plywood, the grain orientation of each layer may be different. The principal grain directions may not coincide with the overall coordinate *x-y* (the right side of Fig. 1). Therefore, in stress analysis, the two sets of stress-strain components must be transformed to the two coordinates system. The two-dimensional stress-strain equation in x-y system is then

$$\begin{Bmatrix} \sigma_x \\ \sigma_y \\ \sigma_{xy} \end{Bmatrix} = [\overline{Q}] \begin{Bmatrix} \varepsilon_x \\ \varepsilon_y \\ \gamma_{xy} \end{Bmatrix} \tag{3}$$

where:

$$[\overline{Q}] = \begin{bmatrix} \cos^2\theta & \sin^2\theta & 2\sin\theta\cos\theta \\ \sin^2\theta & \cos^2\theta & -2\sin\theta\cos\theta \\ -\sin\theta\cos\theta & \sin\theta\cos\theta & \cos^2\theta - \sin^2\theta \end{bmatrix}^{-1} [Q] \begin{bmatrix} \cos^2\theta & \sin^2\theta & \sin\theta\cos\theta \\ \sin^2\theta & \cos^2\theta & -\sin\theta\cos\theta \\ -2\sin\theta\cos\theta & 2\sin\theta\cos\theta & \cos^2\theta - \sin^2\theta \end{bmatrix} \tag{4}$$

A layered composite consists of a number of laminae with different orintations in the thickness direction. To establish a constitutive equation for the composite, the stress and strain components of each layer must be transformed to the global x-y coordinates. For a uniform composite plate with thickness of *h*, the plate resultant forces $\{N\}$ and moments $\{M\}$ are defined by

$$\begin{Bmatrix} N_x \\ N_y \\ N_{xx} \end{Bmatrix} = \int_{-h/2}^{h/2} \begin{Bmatrix} \sigma_x \\ \sigma_y \\ \sigma_{xy} \end{Bmatrix} dz \tag{5}$$

and

$$\begin{Bmatrix} M_x \\ M_y \\ M_{xx} \end{Bmatrix} = \int_{-h/2}^{h/2} \begin{Bmatrix} \sigma_x \\ \sigma_y \\ \sigma_{xy} \end{Bmatrix} z dz \tag{6}$$

where ***z*** is in the thickness direction. When a composite plate consists of *n* thin layers where each layer has different properties, the plate resultant forces and moments will be summations of resultant forces and moments of each layer, respectively. Assuming the *i*th layer located at thickness region from $z = z_{i-1}$ to $z = z_i$, the plate resultant forces and moments of a composite with *n* layers will become:

$$\begin{Bmatrix} N_x \\ N_y \\ N_{xx} \end{Bmatrix} = \sum_{i=1}^{n} \int_{z_{i-1}}^{z_i} \begin{Bmatrix} \sigma_x \\ \sigma_y \\ \sigma_{xy} \end{Bmatrix}_i dz \tag{7}$$

and

$$\begin{Bmatrix} M_x \\ M_y \\ M_{xx} \end{Bmatrix} = \sum_{i=1}^{n} \int_{z_{i-1}}^{z_i} \begin{Bmatrix} \sigma_x \\ \sigma_y \\ \sigma_{xy} \end{Bmatrix}_i zdz \tag{8}$$

Equation (3) describes relationship between stresses and strains in the global x-y coordinate for a laminate. Due to the plate resultant forces and moments, the strains in the laminate include two major components. One is the in-plane strains including ε_x^0, ε_y^0 and γ_{xy}^0. The other is out-plane strain due to the bending with the curvatures of k_x, k_y and k_{xy} (Beer and Johnston 1992). The equation (3) is then

$$\begin{Bmatrix} \sigma_x \\ \sigma_y \\ \sigma_{xy} \end{Bmatrix} = [\overline{Q}] \left(\begin{Bmatrix} \varepsilon_x^0 \\ \varepsilon_y^0 \\ \varepsilon_{xy}^0 \end{Bmatrix} + z \begin{Bmatrix} \kappa_x \\ \kappa_y \\ \kappa_{xy} \end{Bmatrix} \right) \tag{9}$$

Substituting equation (9) to equations (7) and (8), we obtain

$$\begin{Bmatrix} N_x \\ N_y \\ N_{xx} \end{Bmatrix} = \sum_{i=1}^{n} [\overline{Q}] \left(\int_{z_{i-1}}^{z_i} \begin{Bmatrix} \varepsilon_x^0 \\ \varepsilon_y^0 \\ \varepsilon_{xy}^0 \end{Bmatrix}_i dz + \int_{z_{i-1}}^{z_i} \begin{Bmatrix} \kappa_x \\ \kappa_y \\ \kappa_{xy} \end{Bmatrix} zdz \right) \tag{10}$$

and

$$\begin{Bmatrix} M_x \\ M_y \\ M_{xx} \end{Bmatrix} = \sum_{i=1}^{n} [\overline{Q}] \left(\int_{z_{i-1}}^{z_i} \begin{Bmatrix} \varepsilon_x^0 \\ \varepsilon_y^0 \\ \varepsilon_{xy}^0 \end{Bmatrix}_i zdz + \int_{z_{i-1}}^{z_i} \begin{Bmatrix} \kappa_x \\ \kappa_y \\ \kappa_{xy} \end{Bmatrix} z^2 dz \right) \tag{11}$$

Since both in-plane and out-of-plane strains are independent of z, the integration in equations (10) and (11) can be performed. The results can be combined into the following form, which is the constitutive equation for the composite.

$$\begin{Bmatrix} N_x \\ N_y \\ N_{xy} \\ M_x \\ M_y \\ M_{xy} \end{Bmatrix} = \begin{bmatrix} A_{11} & A_{12} & A_{16} & B_{11} & B_{12} & B_{16} \\ A_{12} & A_{22} & A_{26} & B_{11} & B_{22} & B_{26} \\ A_{16} & A_{26} & A_{66} & B_{16} & B_{26} & B_{66} \\ B_{11} & B_{12} & B_{16} & D_{11} & D_{12} & D_{16} \\ B_{12} & B_{22} & B_{26} & D_{12} & D_{22} & D_{26} \\ B_{16} & B_{26} & B_{66} & D_{16} & D_{26} & D_{66} \end{bmatrix} \begin{Bmatrix} \varepsilon_x^0 \\ \varepsilon_y^0 \\ \gamma_{xy}^0 \\ \kappa_x^0 \\ \kappa_y^0 \\ \kappa_{xy}^0 \end{Bmatrix} \tag{12}$$

In addition to the external stresses (i.e., self-weight or restraint), wood composites sometimes have experienced significant internal stresses due to thermal changes and moisture movements. Including the internal stresses, equation (12) becomes

$$\begin{Bmatrix} N_x \\ N_y \\ N_{xy} \\ M_x \\ M_y \\ M_{xy} \end{Bmatrix} + \begin{Bmatrix} N_x^T \\ N_y^T \\ N_{xy}^T \\ M_x^T \\ M_y^T \\ M_{xy}^T \end{Bmatrix} + \begin{Bmatrix} N_x^H \\ N_y^H \\ N_{xy}^H \\ M_x^H \\ M_y^H \\ M_{xy}^H \end{Bmatrix} = \begin{bmatrix} A_{11} & A_{12} & A_{16} & B_{11} & B_{12} & B_{16} \\ A_{12} & A_{22} & A_{26} & B_{11} & B_{22} & B_{26} \\ A_{16} & A_{26} & A_{66} & B_{16} & B_{26} & B_{66} \\ B_{11} & B_{12} & B_{16} & D_{11} & D_{12} & D_{16} \\ B_{12} & B_{22} & B_{26} & D_{12} & D_{22} & D_{26} \\ B_{16} & B_{26} & B_{66} & D_{16} & D_{26} & D_{66} \end{bmatrix} \begin{Bmatrix} \varepsilon_x^0 \\ \varepsilon_y^0 \\ \gamma_{xy}^0 \\ \kappa_x^0 \\ \kappa_y^0 \\ \kappa_{xy}^0 \end{Bmatrix} \tag{13}$$

Symbolically, equation (13) is expressed in the following form:

$$\begin{Bmatrix} N \\ M \end{Bmatrix} + \begin{Bmatrix} N^T \\ M^T \end{Bmatrix} + \begin{Bmatrix} N^H \\ M^H \end{Bmatrix} = \begin{bmatrix} A & B \\ B & D \end{bmatrix} \begin{Bmatrix} \varepsilon^0 \\ \kappa^0 \end{Bmatrix} \tag{14}$$

where {N} are the plate resultant external forces; $\{M\}$ are the plate resultant external moments; $\{\varepsilon^0\}$ are the in-plane strains; $\{k^0\}$ are the curvatures of the mid-surface, and

$$A_{jk} = \sum_{i=1}^{n} \overline{Q}_{jk}^{(i)} t_i \tag{15}$$

$$B_{jk} = \sum_{i=1}^{n} \overline{Q}_{jk}^{(i)} t_i z_i \tag{16}$$

$$D_{jk} = \sum_{i=1}^{n} \overline{Q}_{jk}^{(i)} (t_i z_i^2 + \frac{t_i^3}{12}) \tag{17}$$

$$\{N^T\} = \Delta T \sum_{i=1}^{n} [\overline{Q}]_i \{\alpha^T\}_i t_i \tag{18}$$

$$\{M^T\} = \Delta T \sum_{i=1}^{n} [\overline{Q}]_i \{\alpha^T\}_i t_i z_i \tag{19}$$

$$\{N^H\} = \Delta H \sum_{i=1}^{n} [\overline{Q}]_i \{\alpha^H\}_i t_i \tag{20}$$

$$\{M^H\} = \Delta H \sum_{i=1}^{n} [\overline{Q}]_k \{\alpha^H\}_i t_i z_i$$

where t_i is the thickness of the ith layer; z_i is the centroid of the ith layer; $\{N^T\}$ and $\{M^T\}$ are the plate internal forces and moments due to change of temperature (ΔT) at thermal expansion coefficient of $\{\alpha^T\}$; {NH} and $\{M^H\}$ are the plate internal forces and moments due to change of moisture content (ΔH) at linear expansion coefficient of $\{\alpha^H\}$.

If both external and internal stresses and moments are determined, the composite plate deformations can be obtained from:

$$\begin{Bmatrix} \varepsilon^0 \\ \kappa^0 \end{Bmatrix} = \begin{bmatrix} A & B \\ B & D \end{bmatrix}^{-1} \begin{Bmatrix} N + N^T + N^H \\ M + M^T + M^H \end{Bmatrix} \tag{22}$$

For most wood composite panels, deformation or dimensional changes are mainly caused by the moisture movements. For free hygroscopical expansion where there is no external stresses and thermal stresses ($\{N\}=\{M\}=\{N^T\}=\{N^T\}=\{0\}$), equation (22) then becomes:

$$\begin{Bmatrix} \varepsilon^0 \\ \kappa^0 \end{Bmatrix} = \begin{bmatrix} A & B \\ B & D \end{bmatrix}^{-1} \begin{Bmatrix} N^H \\ M^H \end{Bmatrix} \tag{23}$$

MATERIAL AND TESTING

Six laminated particleboard panels (508- x 508-mm) consisted of three different wood materials were laminated in this study. The panel construction included 4 mm thick sugar maple veneer as the surface layer, 12.7 mm thick particle board (which was commercially available at a local store) as the core layer, and 2 mm thick yellow poplar veneer as the back

layer. All materials were conditioned at 50% relative humidity (RH) and temperature of 20 °C. A commercial epoxy resin was used to form a uniform glue line between the layers. All panels were cold-pressed under about 100 psi for 24 hours to minimize the moisture change and the initial development of unbalanced stresses. After construction, all panels were conditioned according to this exposure schedule: 50% RH to 80% RH to 50% RH to 30% RH. Equilibrium at each RH condition was reached by monitoring weights of selected samples. Their center deflections (warping) were then measured (Fig. 2).

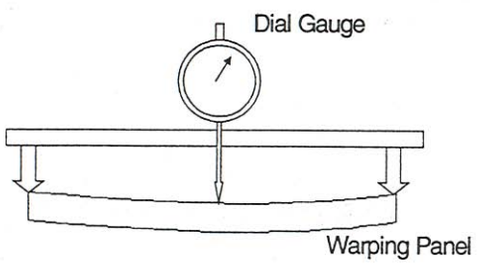

Figure 2 - Measurement of panel warp.

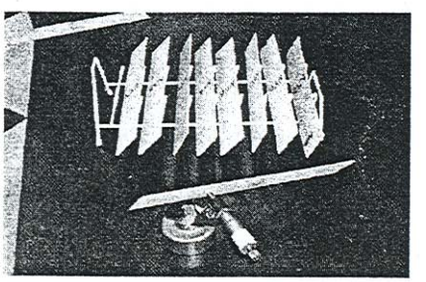

Figure 3 - Sliced layers of particleboard

Particleboard is usually considered as a multi-layer wood composite. Each layer has its own physical properties that might be different from the others'. In order to estimate the physical properties of each layer, particleboards purchased from a local store were ripped into five layers using a band saw (Fig. 3). The sliced particleboards were then placed in an environment chamber and exposed to a sequence of RH conditions: 30% RH to 50% RH to 80% RH to 50% RH to 30RH. The equilibrium MC and linear expansion coefficients were tested according to ASTM 1037. MOE values of veneers and sliced layers of particleboard were determined using stress wave technique. The shear modulus and Poisson Ratios were estimated from the Wood Handbook Forest Products Laboratory 1999).

RESULTS AND DISCUSSIONS

The Particleboard panel exhibit different properties in the thickness direction due to its forming and hot-pressing process. The vertical density profile usually shows high density in the face layers and low density in the core layers. It is believed that the mechanical properties are quite different through the layers. However, the hygroscopic performance of each layer within the particleboard is very limited in the literature. Figure 4 shows typical distributions of the equilibrium moisture contents (EMC) of the sliced layers of particleboard at different relative humidity. The figure also shows the overall EMC of the corresponding particleboard which was tested as whole pieces without slicing. The EMCs of almost all sliced layers are higher than the overall EMC of the particleboard due to more exposure surfaces. It was observed that the equilibrium moisture contents of particleboard through its thickness direction are neither uniform nor symmetry as they have been assumed. The EMCs in the core layers were higher than these in the face layers. And the EMC on both faces were not necessarily the same which would cause the potential warping when being exposed in different environments. The reasons could be the uneven sanding and high density in the face layers which may have reduced the hygroscopicity of the wood particles (Kelly, 1977). Comparison between the adsorption (50% RH - adsorption) and desorption (50% RH - desorption) isotherms indicated the sorption hysteresis which increases the complexity of warping analysis.

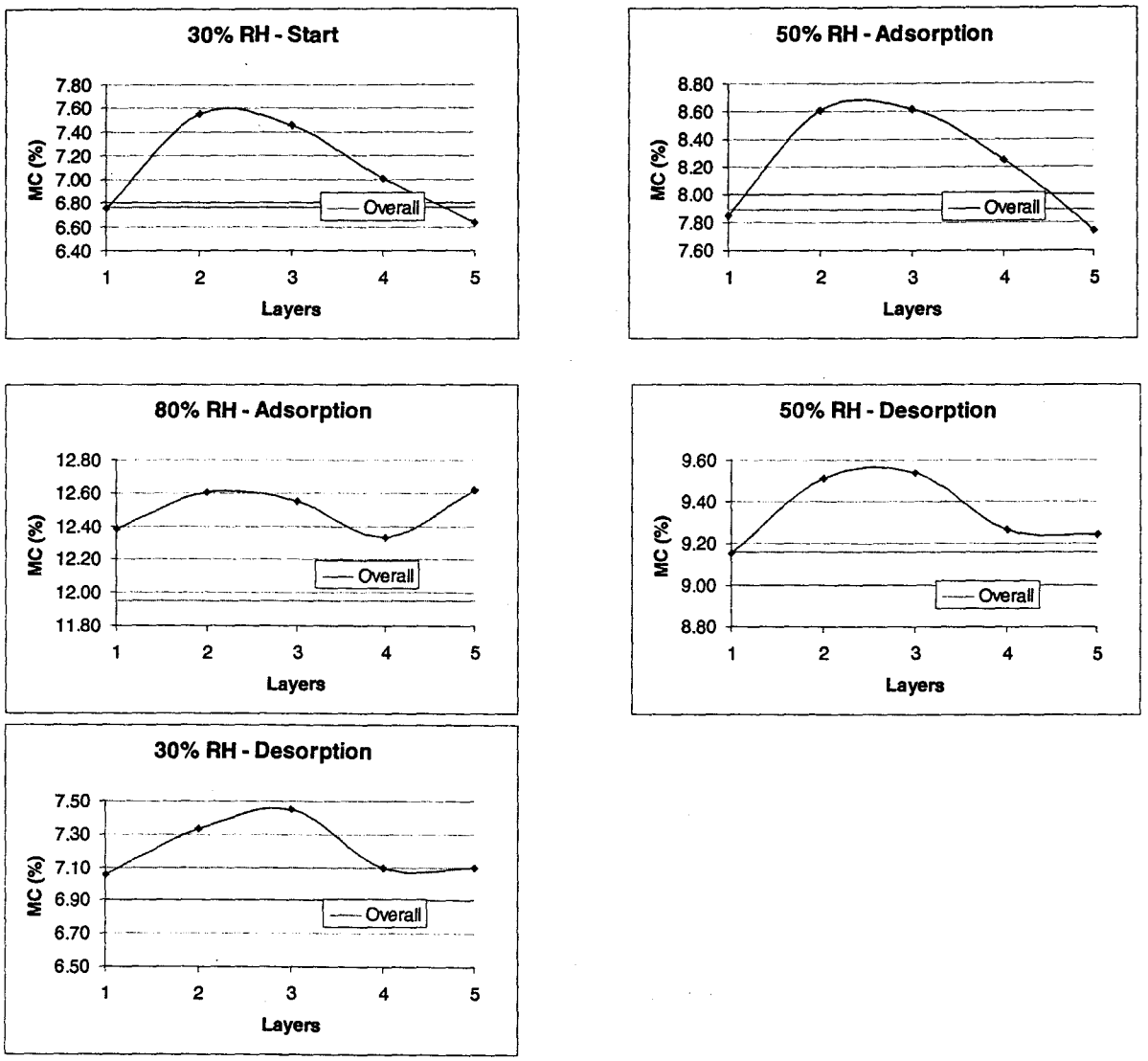

Figure 4 - Typical equilibrium moisture contents of the scliced layers of particleboard at different relative humidity. Overall indicates the moisture content of the corresponding particleboard without slicing.

The linear expansion coefficients of the sliced layers of the particleboard in two different directions under adsorption and desorption are shown in Figure 5. The LEC of particleboards in different hygroscopic processes (adsorption and desorption) may not be necessarily the identical. The upper figure in Figure 5 shows the LECs of the sliced particleboard layers (parallel to the sander mark) under desorption are higher than the ones under adsorption, but the lower figure shows some exceptions. Generally speaking, there is a huge variation (up to 300%) in determining the LEC for the different layers. Furthermore, There is no significant difference of LEC between the face and core layers.

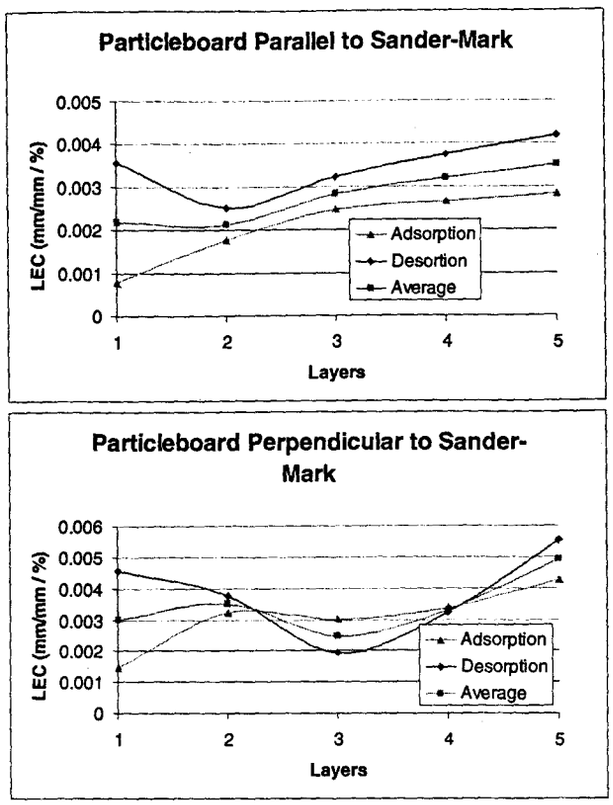

Figure 5 - Typical linear expansion coefficient (LEC) of the sliced layers of the particleboard in two different directions.

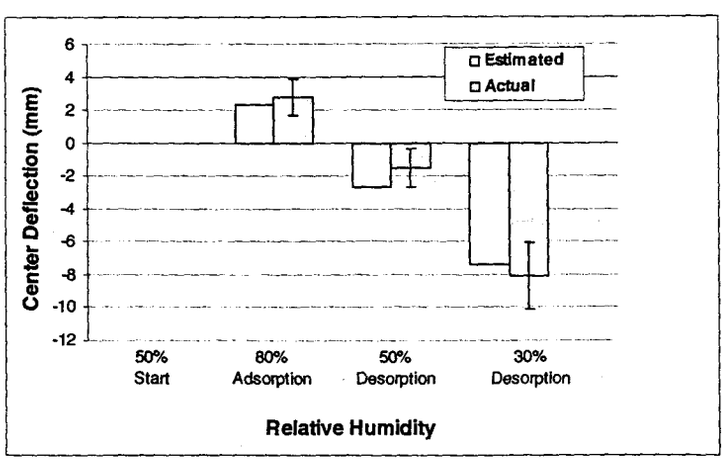

Figure 6 - Estimated and actual warping of the laminated particleboards.

The average properties of each layer and the face veneers for estimating warping are given in Table 1. The warping is quantitatively determined in terms of the center deflection over 508-x 508-mm area. The estimated warping and the actual warping measurements along with their standard deviations are shown in Figure 6. Both estimated and actual warping were performed on the laminated panels with sugar maple veneer (4 mm thick) as the top face layer, particle board (12.7 mm thick) as the core layer, and yellow poplar veneer (2 mm thick) as the bottom layer. The positive center deflections indicate that the panels deform in a convex configuration while the negative center deflections represent panels deformed in a concave form. The horizontal axis shows the sequence of environmental conditions in which the

laminated panels were equilibrated. The panels were constructed at 50% RH under cold pressing and it was assumed that there were no internal unbalanced stresses developed. Therefore, the panels remained flat. After being equilibrated in 80% RH, the unbalanced internal stresses were developed due to different elongations through the thickness. Since the top face (sugar maple veneer) expanded more than the other layers, the whole panels deformed in convex form. When the panels were equilibrated under their initial condition (50% RH) they could no longer be back to their initial flatness. The reason was that the different sorption hysteresis between the wood veneers and particleboard layers resulted the different expansions among them. A large variation in measuring the actual warp was observed because of the variations in their properties and small changes in the EMCs. However, five out of the six laminated panels exhibited the concave deformations which were in accord with the estimated warping. When the panels were equilibrated under 30% RH, the elevated difference in the EMC among the layers increases the internal unbalanced stressed which produced high warping. Again, the dominant shrinkage in the top face layer made the panel warping in a concave form. In all three scenarios the estimated warping performances agreed fairly well with the experimental results.

Table 1 - Average properties of each layer for estimating the warping performance

Layers		Thickness [mm]	E_1[1] [GPa]	E_2[1] [GPa]	G_{12}[2] (MPa)	V_{12}[3]	LEC_1[4] [in./in. %]	LEC_2[4] [in./in. %]	EMC[5] [%] 30% RH	50% RH	80%RH	50%RH	30%RH
Surface (Sugar Maple)		4.00	13.86	1.83	17.71	0.42	1.5E-04	3.3E-03	6.22	9.25	16.04	9.50	6.39
Core (Particleboard)	1	2.54	3.10	2.67	0.55	0.30	2.2E-03	3.0E-03	6.95	7.98	12.35	9.29	7.17
	2	2.54	2.72	2.55	0.55	0.30	2.1E-03	3.5E-03	7.57	8.54	12.59	9.69	7.48
	3	2.54	2.20	2.23	0.55	0.30	2.8E-03	2.5E-03	7.45	8.42	12.40	9.49	7.34
	4	2.54	2.66	2.33	0.55	0.30	3.2E-03	3.3E-03	7.23	8.28	12.45	9.40	7.37
	5	2.54	2.95	2.91	0.55	0.30	3.5E-03	4.9E-03	6.92	7.82	12.65	9.47	7.21
Bottom (Yellow Poplar)		2.00	11.99	1.10	9.02	0.32	2.3E-04	2.7E-03	5.96	8.82	16.53	9.46	6.60

[1] E_1 is MOE value in grain (or sander mark) direction and E, is MOE value perpendicular to the grain (or sander mark) direction.

[2] G_{12} = In-plane shear modulus estimated from Wood Hand Book.

[3] V_{12} = Poisson ration estimated from Wood Hand Book.

[4] LEC = linear expansion coefficient.

[5] EMC = equilibrium moisture content at different relative humidities.

It is important to determine how the input parameters described above will affect dimensional stability and panel warping. Unfortunately, designing an experiment to determine empirical relationships between input parameters and warp is a difficult task. Although the new warping model cannot always predict the exact causes of a particular warping problem due to the uncertainty of material properties, it appears to be a useful tool to better understand the very complex phenomenon. Computer simulations based on the warp model could be used to illustrate the effects of a number of variables (i.e., MC, thickness, MOE, and LE) and identify the most important ones. Figure 7, for an example, shows panel thickness effect on the warping under a particular warping condition. Computer simulation is performed on a 1200 x 2400 –mmboard with assumption that other board characteristics be held constant during repeated simulations. The result exhibits a hyperbolic relationship between the warping and panel thickness with rapidly increasing center deflection below a certain panel thickness. This relationship will provide manufacturers a tool to estimate how thick the panel will be produced to satisfy the required warp performance.

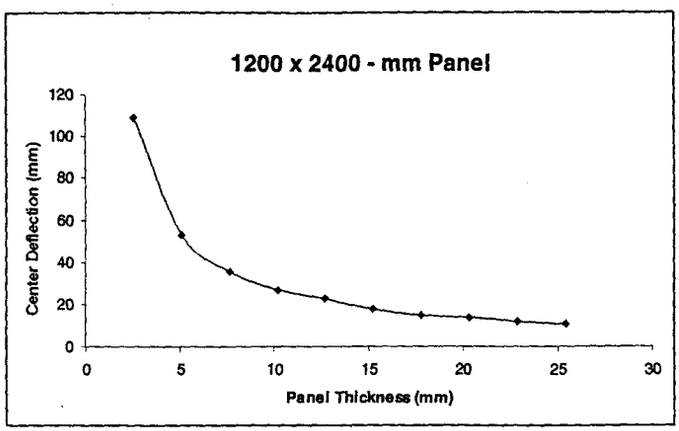

Figure 7 - Thickness effect on warp.

SUMMARY AND CONCLUSIONS

Wood composite under the influence of a moisture gradient is modeled as a layered composite material. Mechanics of layered composites was used to investigate warping of wood composite panels, and a new two-dimensional warping model was introduced. Six laminated particleboard panels were constructed and placed in different relative humidity to evaluate the warping behavior. The experimental results indicated that the equilibrium moisture contents of particleboard through its thickness direction are neither uniform nor symmetry due to the uneven sanding and high density in the face layers. However, .no significant differences of linear expansion coefficients between the face and core layers within particleboard were observed. In all three scenarios of the panel warping tests, the estimated warping performances based on the new warping model agreed fairly well with the experimental results. Although the new warping model could not always predict the exact causes of a particular warping problem due to the uncertainty of material properties, it appeared to be a useful tool to better understand the very complex warping phenomenon.

REFERENCE

Beer, F.P. and E.R. Johnston. 1992. Mechanics of Materials. Second Edition. McGraw-Hill, Inc.

Cloutier, A., G. Gendron., P. Blanchet, S. Ganev., and R. Beauregard. 2001. Finite element modeling of dimensional stability in layered wood composites. 35th International Particleboard/Composite Materials Symposium, Washington State University, Pullman, WA. April 3-5, 2001, p18.

Forest Products Laboratory. 1999. Wood handbook--Wood as an engineering material. Gen. Tech. Rep. FPL-GTR-113. Madison, WI: U.S. Department of Agriculture, Forest Service, Forest Products Laboratory.

Heebink, B.C., and H.H. Haskell. 1962. Effect of heat and humidity on the properties of high pressure laminates. Forest Prod. J. 20(11):542-548.

Heebink, B.G., E.W. Kuenzi and A.C. Maki. 1964. Linear movement of plywood and flakeboards as related to the longitudinal movement of wood. Forest Service Research Report FPL-073.

Kelly, M.W. 1977. Critical literature review of relationships between processing parameters and physical properties of particleboard. Gen. Tech. Rep. FPL-GTP-10. Madison, WI : U.S. Department of Agriculture, Forest Products laboratory.

National Particleboard Association. 1996. Standard method for measurement of warp in particleboard and medium density fiberboard. NPA, 18928 Premiere Court, Gaithersburg, MD, 20879.

Norris, C.B. 1964. Warpage of laminated materials due to change in moisture content or temperature. Appendix in: Heebink, B.G., E.W. Kuenzi and A.C. Maki. 1964. Linear movement of plywood and flakeboards as related to the longitudinal movement of wood. Forest Service Research Report FPL-073.

Suchsland, O., and J.D. McNatt. 1986. Computer simulation of laminated wood panel warping. Forest Prod. J. 36(11/12):16-23.

Suchsland, O. 1990. Estimating the warping of veneered furniture panels. Forest Prod. J. 40(9):39-43.

Suchsland, O., Y. Feng, and D. Xu. 1993. The warping of laminated particleboard. Wood Science Series, No. 4. Department of Forestry, Michigan State University, East Lansing, MI.

Suchsland, O., Y. Feng, and D. Xu. 1995. The hygroscopic warping of laminated panels. Forest Prod. J. 45(10): 57-63.

Sun, C.T. 1994. Mechanics of composite materials and laminates. Lecture notes for AAE 555. School of Aeronautics and Astronautics, Purdue University, West Lafayette, IN.

Tong, Y., and O. Suchsland. 1993. Application of finite element analysis to panel warping. Holz Roh- u. Werkstoff. 51(1): 55-57.

Wu, Q. 1999. Application of Nelson's sorption isotherm to wood composites and overlays. Wood Fiber Science 31(2):187-191.

The 7th Pacific Rim Bio-Based Composites Symposium

PROCEEDINGS

Volume II

Nanjing, China
October 31 - November 2
2004